Vertical plasmonic slot lithium niobate Mach-Zehnder modulator

1st Jihao Zhao
Wuhan National Laboratory for Optoelectronics & School of Optical and Electronic Information
Huazhong University of Science and Technology
Wuhan, China

2nd Yilun Wang*
Wuhan National Laboratory for Optoelectronics & School of Optical and Electronic Information
Huazhong University of Science and Technology
Wuhan, China

3rd Liao Chen
Wuhan National Laboratory for Optoelectronics & School of Optical and Electronic Information
Huazhong University of Science and Technology
Wuhan, China

4th Chi Zhang
Wuhan National Laboratory for Optoelectronics & School of Optical and Electronic Information
Huazhong University of Science and Technology
Wuhan, China

5th Xinliang Zhang*
Wuhan National Laboratory for Optoelectronics & School of Optical and Electronic Information
Huazhong University of Science and Technology
Wuhan, China

*Corresponding authors:
ylwang@hust.edu.cn;
xlzhang@mail.hust.edu.cn

***Abstract*—We demonstrate an ultra-compact and high-efficiency lithium niobate Mach-Zehnder modulator enabled by two vertical plasmonic slot waveguides, which shows a half-wave voltage-length product of 0.042 Vcm and a theoretical bandwidth exceeding 1.4 THz.**

Keywords*—*Plasmonics, Mach-Zehnder modulator, Lithium niobate

I. INTRODUCTION

High-performance Mach-Zehnder modulator (MZM) is the critical device to meet the growing demands of the global data traffic. Lithium niobate (LN) is one of the most commonly used electro-optic materials for MZM due to its outstanding properties, such as good and stable electro-optic activity, linear performance, and low optical loss. Thin-film LN MZM enables high-speed and compact structure [1], but the modulation efficiency is still relatively low because of the fundamental limitations of the overlap between the optical and electric fields. Plasmonic technology is a good solution to overcome this problem for the LN MZM [2]. However, in the previous structure, the confinement of the optical and electric fields in the vertical direction can be further improved for higher efficiency. The vertical plasmonic slot waveguide is a promising method to further enhance the confinement and the achievable overlap of the corresponding fields, leading to extremely high modulation efficiency [3]. Here, we utilize vertical gold-LN-gold structures for the plasmonic LN MZM. Due to the extreme field confinement and ultra-low capacitance of the proposed structure, it enables an active length of 15 µm, a modulation efficiency of 0.042 Vcm and a theoretical bandwidth of 1.4 THz. Moreover, the proposed MZM operates near its quadrature point by designing the width of the two interferometric arms for high linearity.

II. DESIGN AND SIMULATION

The proposed vertical plasmonic slot LN MZM is designed on the Z-cut LN-on-insulator platform with a 100-nm-thick LN top layer, a 4.7-µm-thick buried oxide layer, and a100-nm-thick gold layer between the LN and the buried oxide layer. An 80-nm-thick gold top layer is deposited on the LN layer to form the plasmonic structures. The schematic diagram of the proposed MZM is shown in Figure 1(a) and the inset. The phase shifters consist of two 15-µm-long vertical plasmonic slot waveguides (PSWs), which can also be used as electrodes. Each vertical PSW consists of a top gold nanowire, a bottom gold layer, and a middle LN layer. The optical signal from the fiber is coupled into the MZM through a metallic grating coupler to form the plasmonic mode, and is split into two phase shifter arms by a Y-branch. After phase modulation is generated by the phase shifters, the signals interfere at opposite Y-branch to achieve intensity modulation and couple out of the MZM through another metallic grating coupler. Note that there are 100-nm-wide air gaps between the Y-branches and the phase shifters to prevent short circuit.

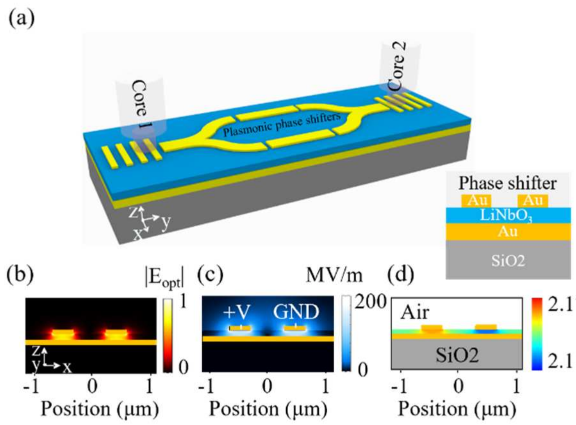

Fig.1. (a) Conceptional image of the vertical plasmonic slot LN MZM, including two metallic grating couplers, Y-branches, and phase shifters. The inset shows the cross-section of the phase shifter, and the plasmonic mode is formed by the vertical slot structure of gold-LN-gold. (b) Optical field of the LN MZM. (c) Electric field of the LN MZM, by adding +V and GND to the electrodes, respectively. (d) The refractive index of the two arms changes in opposite directions by the Pockels effect, realizing the push-pull operation.

As shown in Figures 1(b) and 1(c), the vertical plasmonic slot structure extremely confines the optical and electric fields in the LN layer, allowing the maximum use of the added radio frequency (RF) signal for modulation. Meanwhile, the distributions of the optical and electric fields are similar, which significantly improves the interaction factor between the corresponding fields to further enhance the modulation efficiency. Figure 1(d) shows that the refractive index of the two optical channels changes oppositely with the electrostatic field applied in opposite directions, realizing the push-pull phase modulation.

The numerical simulations of the modulation efficiency and the optical losses of the MZM are acquired by using a commercial finite element method solver (Comsol Multiphysics 5.5). For the electrostatic simulations, the cross-section of the two phase shifters is modelled with the relative permittivity $\epsilon_{air} = 1$ of air and the strain-free static relative permittivity tensor of LN ($\epsilon_{xx} = \epsilon_{yy} = 84.5$, $\epsilon_{zz} = 27.8$) taken from Jazbinsek et al. [4]. The electrostatic field distribution E(x,z) in the phase shifters is calculated with two upper gold electrodes applied +V and GND, respectively. The electro-optically induced birefringence in LN ($r_{zzz} = 31.45$ pm/V, $r_{xxz} = r_{yyz} = 10.12$ pm/V) is calculated by using the Pockels coefficients from Jazbinsek et al. [4]. The optical mode analysis is calculated by considering the lateral distribution of the electro-optically modified refractive index of the structure, while the refractive indices of Au and LN are taken from Johnson and Christy [5] and Zelmon et al. [6] ($n_{xx} = n_{yy} = n_o = 2.211$, $n_{zz} = n_e = 2.138$ at $\lambda_0 = 1550$ nm). The modulation efficiency of different structures is calculated by adding a certain voltage to change the effective refractive index of the optical mode.

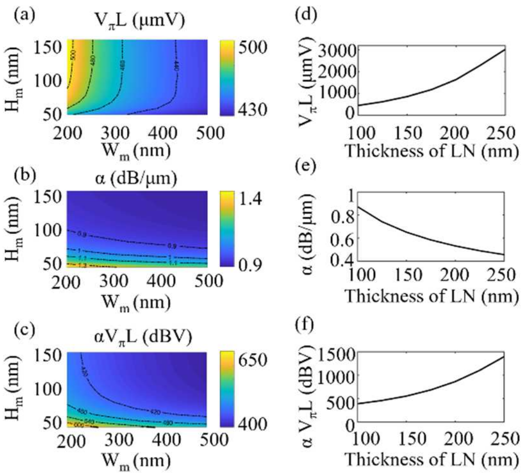

Fig.2. (a)(b)(c) Modulation efficiency, optical loss, and their multiplication as a function of the height (H_m) and width (W_m) of the top gold nanowires. (d)(e)(f) Modulation efficiency, optical loss, and their multiplication as a function of the thickness of LN.

As seen in Figure 2(a), sweeping the structural parameters of the top gold nanowires in the phase shifters to achieve higher modulation efficiency, it can be obtained that the height has a small effect on the modulation efficiency, while the width plays a major role. The modulation efficiency improves with width increasing and remains almost unchanged after a certain width is exceeded. Figure 2(b) shows that the height (H_m) should be higher than 60 nm to reduce optical loss (α). Considering both the modulation efficiency and the propagation loss of the modulators, the loss-half-wave-voltage-length product $\alpha V_\pi L$ is utilized to describe the overall performance of the MZM. To obtain low loss and low voltage for the practical application, the H_m and W_m should be large for a low $\alpha V_\pi L$ as shown in Figure 2(c). Besides, the thickness of the LN layer is also significant for the overall performance of MZM. In Figure 2(d), $V_\pi L$ is nearly linearly proportional to the thickness of the LN layer. It means that the modulation efficiency improves with the thickness decreasing. However, the trend of optical loss is completely opposite to that of the modulation efficiency as shown in Figure 2(e). Fortunately, the $\alpha V_\pi L$ can help to choose the appropriate thickness of the LN layer in Figure 2(f). Finally, the height of the top gold nanowires is chosen to be 80 nm, and the thickness of the lithium niobate is chosen to be 100 nm. The width of the two gold nanowires needs to be designed for the high-linearity operation as follows.

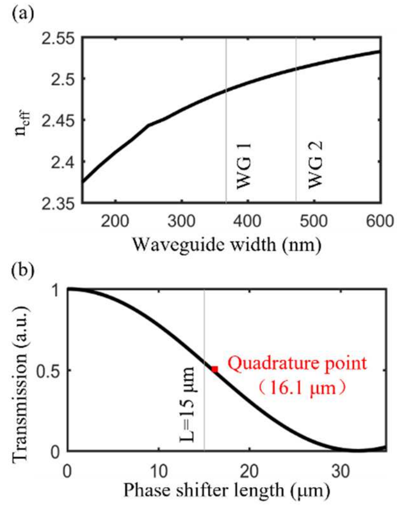

Fig.3. (a) Mode effective index n_{eff} as a function of the gold nanowire width. (b) Transfer function for the MZM with phase-shifter length.

In order to operate the modulator at the quadrature point, the effective mode refractive index of the two arms of the modulator needs to be designed differently to introduce the initial phase difference. As shown in Figure 3(a), the effective mode refractive index increases with gold nanowire width increasing, and the widths of the two gold nanowires are taken to be 375 nm and 475 nm, respectively. Considering the effects of the bandwidth and the optical loss, and to make the MZM operate near the quadrature point, the length of the phase shifters is chosen to be 15 μm as shown in Figure 3 (b). The calculated $V_\pi L$ of this structure is 0.078 Vcm for the 375-nm-wide waveguide and 0.091 Vcm for the 475-nm-wide waveguide, thus the $V_\pi L$ of the device is reduced to 0.042 Vcm in push-pull mode. The calculated $V_\pi L$ is slightly different from that in Figure 2, because the widths of the waveguides in Figure 2 are the same while the widths of the waveguides in this structure are different.

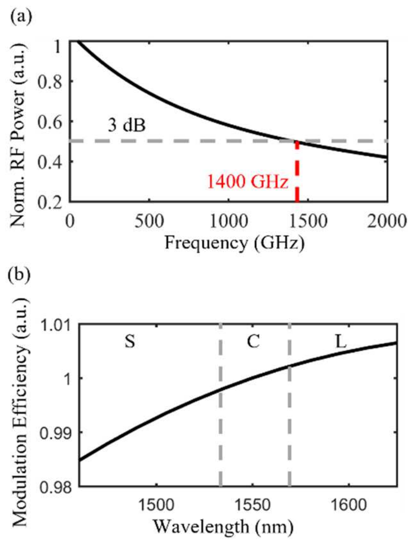

Fig.4. (a) Normalized RF power as a function of the frequency. (b) Modulation efficiency as a function of wavelength, normalized by the modulation efficiency at the wavelength of 1550 nm.

The Figure 4(a) shows the simulated bandwidth of the proposed MZM, taking into account the modulator light speed and RF speed matching, RF loss, impedance matching, etc [7]. The theoretical 3-dB bandwidth of the MZM can reach 1.4 THz. Figure 4(b) shows the spectral broadband operation over the telecom wavelength bands S, C and L (1460-1625 nm) with <1 dB modulation depth variation. The slight variations observed are caused by the wavelength dependence of the optical field and the shift of the operating point in the transfer function.

III. Conclusions

We designed and demonstrated a high-efficiency LN MZM with a half-wave voltage-length product of 0.042 Vcm and the theoretical 3-dB bandwidth can reach 1.4 THz. Due to the design of the waveguide widths, the modulator operates close to its quadrature point with high linearity. Moreover, the modulator operates over the telecom wavelength bands with <1 dB modulation depth variation.

Acknowledgment

This research was funded by the National Natural Science Foundation of China (Grant Nos. 61927817) and China Postdoctoral Science Foundation (BX20220123, 2022M720051).

References

[1] C. Wang et al., “Integrated lithium niobate electro-optic modulators operating at CMOS-compatible voltages,” Nature, vol. 562, pp. 101-104, September 2018.

[2] M. Thomaschewski, sV. A. Zenin, S. Fiedler, C. Wolff, S. I. Bozhevolnyi, “Plasmonic Lithium Niobate Mach−Zehnder Modulators,” Nano Lett., vol. 22, pp. 6471-6475, August 2022.

[3] A. Messner et al., “Broadband Metallic Fiber-to-Chip Couplers and a Low-Complexity Integrated Plasmonic Platform,” Nano Lett, vol. 21, pp. 4539-4545, June 2021.

[4] M. Jazbinsek, M. Zgonik, “Material tensor parameters of LiNbO3 relevant for electro- and elasto optics,” Appl. Phys. B, vol. 74, pp. 407−414, April 2022.

[5] P. B. Johnson, R. W. Christy, “Optical constants of the noble metals,” Phys. Rev. B, vol. 6, pp. 4370-4379, December 1972.

[6] D. E. Zelmon, D. L. Small, D. Jundt, “Infrared corrected Sellmeier coefficients for congruently grown lithium niobate and 5 mol.% magnesium oxide−doped lithium niobate,” J. Opt. Soc. Am. B, vol. 14, pp. 3319-3322, December 1997.

[7] A. Honardoost, R. Safian, A. Rao, S. Fathpour, “High-Speed Modeling of Ultracompact Electrooptic Modulators,” J. Light. Technol., vol. 36, pp. 5893-5902, December 2018.